Extragalactic source counts in the Spitzer 24 micron band: what do we expect from ISOCAM 15 micron data and models?

Article (Published Version)

The Astrophysical Journal, 618:L9–L12, 2005 January 1

EXTRAGALACTIC SOURCE COUNTS IN THE *SPITZER* 24 MICRON BAND: WHAT DO WE EXPECT FROM ISOCAM 15 MICRON DATA AND MODELS?

C. Gruppioni,[1] F. Pozzi,[2] C. Lari,[3] S. Oliver,[4] and G. Rodighiero[5]
Received 2004 September 7; accepted 2004 November 18; published 2004 November 29

ABSTRACT

The comparison between the new *Spitzer* data at 24 μm and the previous ISOCAM data at 15 μm is a key tool to understand galaxy properties and evolution in the infrared and to interpret the observed number counts, since the combination of *Spitzer* with the *Infrared Space Observatory* cosmological surveys provides for the first time the direct view of the universe in the infrared up to $z \gtrsim 2$. We present the prediction in the *Spitzer* 24 μm band of a phenomenological model for galaxy evolution derived from the 15 μm data. Without any "a posteriori" update, the model predictions seem to agree well with the recently published 24 μm extragalactic source counts, suggesting that the peak in the 24 μm counts is dominated by "starburst" galaxies like those detected by ISOCAM at 15 μm but at higher redshifts ($1 \lesssim z \lesssim 2$ instead of $0.5 \lesssim z \lesssim 1.5$).

Subject headings: cosmology: observations — galaxies: evolution — galaxies: starburst — infrared: galaxies

1. INTRODUCTION

Cosmological constraints on the evolution of galaxies have been recently investigated by studying the statistical properties of large samples. In particular, the combined analysis of extragalactic source counts and redshift distributions is generally used to calibrate the theoretical models as a function of time. The mid-infrared (MIR) and far-infrared (FIR) regions of the electromagnetic spectrum probe the population of actively star-forming galaxies obscured by dust. Extragalactic source counts from different surveys over a wide flux range obtained with the ISOCAM instrument on board the *Infrared Space Observatory* (*ISO*) indicate that these sources have evolved rapidly, significantly faster than deduced from optical surveys (Elbaz et al. 1999; Gruppioni et al. 2002; Metcalfe et al. 2003; Rodighiero et al. 2004). These results are supported by the detection of a substantial cosmic infrared background (CIRB; Hauser & Dwek 2001), which is interpreted as the integrated emission from dust present in galaxies. The contribution of resolved ISOCAM sources accounts for ~60%–70% of the CIRB at MIR frequencies, the bulk of this background originating in discrete sources at $z \lesssim 1.2$ (Franceschini et al. 2001; Elbaz et al. 2002).

The *Spitzer Space Telescope* is now providing new insights into the IR population contributing to the CIRB, in particular with the Multiband Imaging Photometer 24 μm band, which is starting to detect a population of galaxies that may be IR-luminous galaxies at $z \sim 1.5$–3 (i.e., high-redshift analogs of the faint 15 μm galaxies detected by ISOCAM; see Chary et al. 2004). Preliminary results from the 24 μm extragalactic source counts (Marleau et al. 2004; Papovich et al. 2004), confirming the existence of the rapidly evolving dust-obscured population discovered by ISOCAM, raise the question of how to compare them with the previous ISOCAM counts at 15 μm. Both 24 and 15 μm bands are extremely sensitive to the presence of broad emission features at 6.2, 7.7, 8.6, 11.3, and 12.7 μm in the spectra of galaxies, probably from polycyclic aromatic hydrocarbons (PAHs; Puget & Leger 1989). Since these features dominate the photometric output at some redshifts, the ratio between the *Spitzer* 24 μm and the ISOCAM 15 μm fluxes ($S_{24\,\mu m}/S_{15\,\mu m}$) is strongly dependent on z. In Figure 1, this ratio versus z is shown for the populations contributing to the MIR source counts (see § 2 for a discussion): "starburst" galaxies (M82 spectral energy distribution [SED]), "normal" galaxies (M51), type 1 active galactic nuclei (AGNs; SED from Elvis et al. 1994), and type 2 AGNs (Circinus). As clearly shown in the plot, the 15 μm band is optimized for detecting $0.5 \lesssim z \lesssim 1.5$ galaxies, while the 24 μm band is favored for the detection of galaxies at $z \gtrsim 1.5$. Since the comparison between the source counts in the two bands is a powerful tool for understanding the evolutionary properties of the different galaxy populations contributing to the counts at different redshifts and flux levels, it is worthwhile performing a careful comparison.

In a recent paper on extragalactic source counts from the First Look Survey (FLS), Marleau et al. (2004) try to compare the 24 μm source counts with the previous 15 μm counts from different ISOCAM surveys, transformed to 24 μm. However, the reported transformation appears to be overly simplistic, since the ISOCAM counts (plotted in Fig. 4 of Marleau et al. 2004) have been converted to the *Spitzer* 24 μm band by considering a single value for the $S_{24\,\mu m}/S_{15\,\mu m}$ flux ratio for all flux densities. The value used by the authors ($S_{24\,\mu m}/S_{15\,\mu m} = 1.2$) is a median value derived from typical luminous infrared galaxy/ultraluminous infrared galaxy SEDs at relatively high z (Chary & Elbaz 2001), which is appropriate only for sources making up the peak of the counts. In fact, as shown in Figure 1, if we consider the starburst template (M82), we obtain a local value for the flux ratio of ~2.5, while we reach a value of ~1.3 only at $z \sim 1$. Therefore, only the contribution to the counts made by galaxies with z around 1 could be transformed to 24 μm using a flux ratio similar to that considered by Marleau et al. (2004). In particular, the bright part of the European Large-Area *ISO* Survey (ELAIS) counts (Gruppioni et al. 2002), linking the *IRAS* counts to the deep ISOCAM counts, is dominated by nearby non-evolving normal galaxies (with ratios of ~1.7) and by starburst galaxies and type 2 AGNs (with ratios of ~2.5 and ~2.3, respectively), as shown by La Franca et al. (2004). Therefore, the

[1] Istituto Nazionale di Astrofisica, Osservatorio Astronomico di Bologna, via Ranzani 1, I-40127 Bologna, Italy; carlotta.gruppioni@bo.astro.it.
[2] Dipartimento di Astronomia, Università di Bologna, via Ranzani 1, I-40127 Bologna, Italy.
[3] Istituto di Radioastronomia del CNR, via Gobetti 101, I-40129 Bologna, Italy.
[4] Astronomy Centre, Department of Physics and Astronomy, University of Sussex, Brighton BN1 9QJ, UK.
[5] Dipartimento di Astronomia, Università di Padova, vicolo dell'Osservatorio 2, I-35122 Padua, Italy.

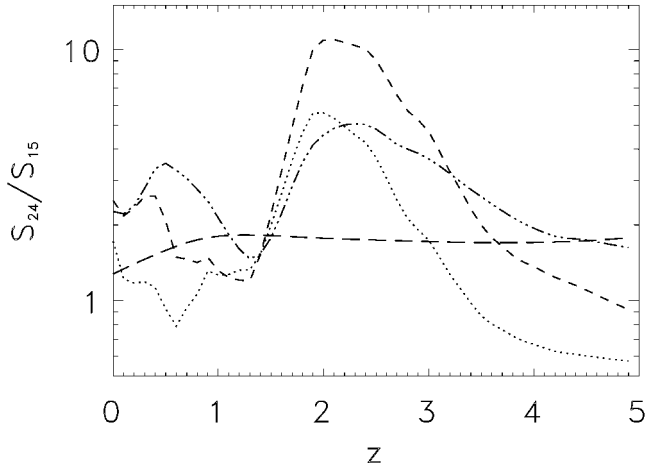

FIG. 1.—$S_{24\,\mu m}/S_{15\,\mu m}$ ratio as a function of redshift for the MIR populations contributing to the observed number counts: starburst galaxies (*short-dashed line*: M82 SED prototype), normal galaxies (*dotted line*: M51), type 2 AGNs (*triple-dot–dashed line*: Circinus), and type 1 AGNs (*long-dashed line*: SED from Elvis et al. 1994).

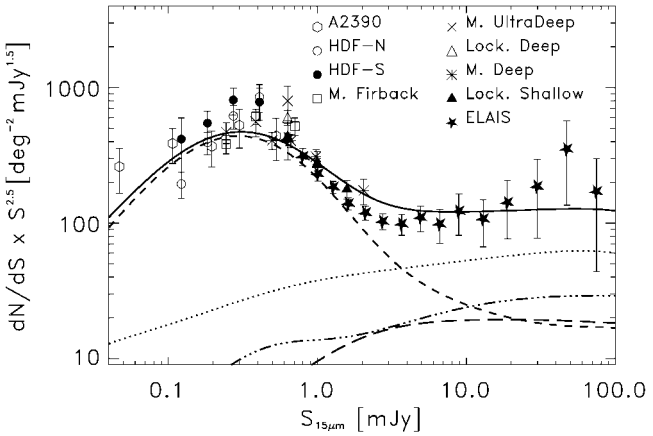

FIG. 2.—Normalized differential source counts in the ISOCAM 15 μm band. As explained in the plot, data points are from several surveys (HDF-N, HDF-S, Marano Firback, ultradeep, and deep: Elbaz et al. 1999; ultradeep lensed: Metcalfe et al. 2003; ELAIS-S1: Gruppioni et al. 2002; Lockman deep and shallow: Rodighiero et al. 2004). The model curves are from Pozzi et al. (2004) for galaxies (*dashed line*: starburst; *dotted line*: normal) and from I. Matute et al. (2005, in preparation) for AGNs (*long-dashed line*: type 1; *triple-dot–dashed line*: type 2).

use of a single ratio value of 1.2 produces a misleading result [especially at $S_{24\,\mu m} > 1$ mJy: i.e., 15 μm counts shifted downward by a factor of $(1.7/1.2)^{1.5}$–$(2.5/1.2)^{1.5} = 1.7$–3.0], suggesting an apparent inconsistency between the bright part of the source counts in the two bands.

Since at the moment there are no large areas with available data at both wavelengths, we can make use of a model fitting the observed 15 μm source counts (Pozzi et al. 2004; I. Matute et al. 2005, in preparation) to transform the counts from one frequency to the other, thus allowing a direct comparison.

In this Letter, we discuss the more realistic way to transform the model predictions and the observed data from the LW3 band of ISOCAM to the 24 μm band of *Spitzer*, in order to compare the properties of the 24 μm sources with those of the ISOCAM 15 μm ones. The Letter is structured as follows: in § 2, we describe the evolutionary model fitting the 15 μm observables; in § 3.1, we show the model predictions at 24 μm; in § 3.2, we discuss a method to transform the observed data points from 15 to 24 μm; in § 4, we present our conclusions.

Throughout this Letter, we assume $H_0 = 75$ km s^{-1} Mpc^{-1}, $\Omega_m = 0.3$, and $\Omega_\Lambda = 0.7$.

2. THE MODEL

The model is based on the first direct determination of the 15 μm luminosity function (LF) of galaxies and AGNs, based on data from the ELAIS southern fields survey (Lari et al. 2001; La Franca et al. 2004; Rowan-Robinson et al. 2004). We assume that four main populations, evolving independently, contribute to the observed source counts: starburst and normal galaxies and type 1 and 2 AGNs. A maximum likelihood analysis (Marshall et al. 1983) has been used to simultaneously fit both evolution rates and shape parameters of the different local LFs. Although AGNs make up a nonnegligible fraction of the extragalactic source counts at 15 μm (especially at high flux densities), galaxies are the dominant class in the MIR.

The LF determination for galaxies, described extensively in Pozzi et al. (2004), is based on a sample of about 150 galaxies in the redshift interval $0.0 \le z \le 0.4$, covering a large flux density range between *IRAS* and the deep ISOCAM surveys (0.5 mJy $\le S_{15\,\mu m} \le$ 50 mJy). The normal, nonevolving, and the starburst, evolving, populations are separated using the new criterion based on the MIR to optical luminosity ratio ($L_{15\,\mu m}/L_R$). We use the basic Silva et al. (1998) models to reproduce the SED of our prototypical galaxies, assumed to be M82 for the starburst population and M51 for the normal one. The MIR region (between 3 and 18 μm) of the modeled spectra were replaced with ISOCAM circular variable filter observations (M82: Förster-Schreiber et al. 2003; M51: Roussel et al. 2001). Note that, for simplicity, we have used a single template SED for each population, instead of different SEDs for different infrared luminosity intervals. While the normal population is consistent with no evolution, for the starburst population a strong evolution is found both in luminosity [$L(z) \propto (1 + z)^{3.5}$ up to $z \sim 1$] and in density [$\rho(z) \propto (1 + z)^{3.8}$ up to $z \sim 1$]. The evolutionary parameters of our model have been tested by comparing the model predictions with all the available observables, like source counts at all flux density levels (from 0.1 to 300 mJy) and redshift distributions and LFs at high z. The agreement between the model predictions and the observed data is remarkably good (see Fig. 2 for an example of how the model fits the observed number counts at 15 μm).

The LF determination for AGNs (both type 1 and 2), described in I. Matute et al. (2005, in preparation), is based on ELAIS data (27 type 1 AGNs and 25 type 2 AGNs) combined with the local *IRAS* sample at 12 μm of Rush et al. (1993), converted to 15 μm using appropriate SEDs (41 type 1 AGNs and 50 type 2 AGNs). The typical SED assumed for type 1 AGNs is that compiled by Elvis et al. (1994), while for type 2 AGNs, two extreme cases of the obscured AGN SED in the MIR were assumed: a starburst-like SED (Circinus; Sturm et al. 2000) and an AGN-like SED (NGC 1068; Sturm et al. 2000). Type 1 AGNs are found to evolve with a luminosity evolution [$L(z) \propto (1 + z)^{k_L}$], with an evolution rate k_L equal to 2.6 up to $z \sim 2$ and constant thereon). A similar evolutionary scenario is found for type 2 AGNs, with k_L ranging from 2.0 to 2.6 depending on the adopted SED (NGC 1068 or Circinus, respectively). The best-fitting model is found to reproduce well both observed source counts and redshift distributions, as shown by I. Matute et al. (2005, in preparation).

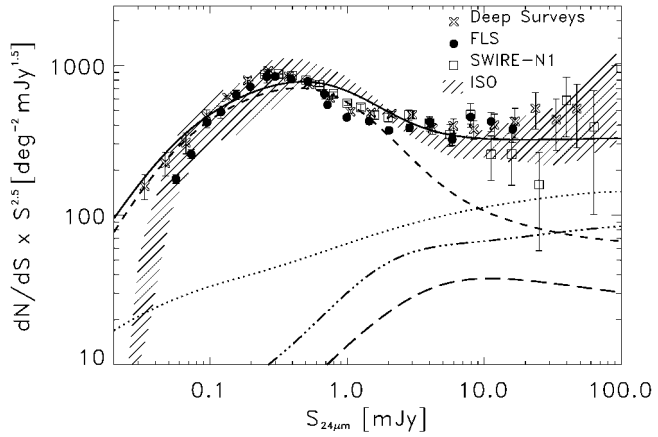

FIG. 3.—Normalized differential source counts at 24 μm (*crosses*: deep *Spitzer* surveys, Papovich et al. 2004; *filled circles*: FLS, Marleau et al. 2004; *open squares*: SWIRE-N1, D. L. Shupe et al. 2005, in preparation) with the model predictions (as in Fig. 2) and the 15 μm data (*hatched region*) transformed to 24 μm as described in the text.

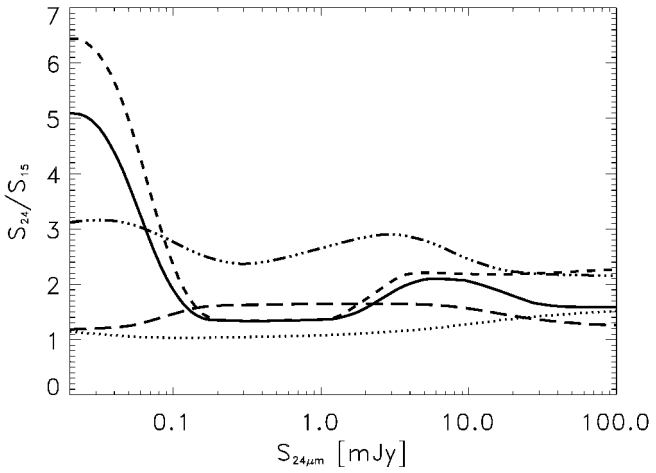

FIG. 4.—Median values of the $S_{24\,\mu m}/S_{15\,\mu m}$ flux density ratio as function of $S_{24\,\mu m}$, as derived by our model for all the populations (weighted mean: *solid line*; different populations: *lines as in previous figures*).

3. COUNTS AT 24 μm

3.1. *Model Predictions at* 24 μm

By using the appropriate SED for each population and convolving the SED with the appropriate filter transmission, the galaxy and AGN local LFs have been transformed from 15 to 24 μm. Then the predicted 24 μm source counts have been computed for all the contributing populations. In Figure 3, the source counts predicted by our model are compared to the recently published *Spitzer* 24 μm data from the FLS (Marleau et al. 2004), from the deep surveys (Papovich et al. 2004), and from the *Spitzer* Wide-Area Infrared Extragalactic Survey (SWIRE; D. L. Shupe et al. 2005, in preparation). We can notice a consistency between data and model, with no need, at least in first approximation, for the use of more extreme SEDs for starburst galaxies (i.e., Arp 220). AGNs (either type 1 or 2) do not dominate the observed source counts at any flux level, although type 2 make about 25% of the counts at $S_{24\,\mu m} > 10$ mJy. The counts are dominated by nonevolving normal galaxies at $\gtrsim$8 mJy and by evolving starburst galaxies at lower flux densities. The assumption made in our model of no evolution for galaxies at $z > 1$, not very well constrained by ISOCAM data, is "a posteriori" consistent with *Spitzer* data.

It is interesting to see how the ratio between the *Spitzer* 24 μm and the ISOCAM 15 μm flux for all the populations changes as a function of z (Fig. 1) and of the 24 μm flux (as derived by our model; Fig. 4). The comparison between Figures 1 and 4 clearly shows that the higher flux densities ($S_{24\,\mu m} > 2$–3 mJy) are dominated by nearby objects with moderately high values of the $S_{24\,\mu m}/S_{15\,\mu m}$ ratio (~2.2: starburst and type 2 AGNs; ~1.7: normal galaxies), while the bump of the 24 μm counts (at fluxes 0.1–1 mJy) is dominated by objects with $S_{24\,\mu m}/S_{15\,\mu m} \approx 1.4$ (mainly starburst galaxies at $0.7 \lesssim z \lesssim 1.5$). These are the same populations found to contribute to the ISOCAM 15 μm source counts. However, since we have approximately

$$\left(\frac{dN}{dS}S^{2.5}\right)_{24\,\mu m} = \left(\frac{dN}{dS}S^{2.5}\right)_{15\,\mu m}\left(\frac{S_{24\,\mu m}}{S_{15\,\mu m}}\right)^{1.5} \qquad (1)$$

and the ratio value at flux densities around the peak of the differential source counts is $\simeq$1.4, the evolutionary excess is more pronounced at 15 μm than at 24 μm. At the lower flux densities ($S_{24\,\mu m} \lesssim 0.1$ mJy), sources with high flux ratio values ($S_{24\,\mu m}/S_{15\,\mu m} > 2.0$–2.5, corresponding to $z > 1.5$) start to dominate the counts. These high-z starburst galaxies, mainly at $1.5 \leq z \leq 2.5$, are not visible in the ISOCAM surveys, because of the 15 μm k-correction, but contribute to the fainter end of the 24 μm source counts and to the 24 μm cosmic background. Since the existence of this starburst population at high redshift is predicted just by extrapolating our 15 μm model to higher z, it is likely that faint 24 μm sources are the high-redshift likes of the fainter 15 μm sources detected by ISOCAM (see also Chary et al. 2004).

The same kind of considerations are evident from Figure 5, where the contributions to the 24 μm number counts from different redshift intervals are shown. While galaxies with $0.0 \lesssim z \lesssim 0.5$ dominate the high fluxes ($S_{24\,\mu m} \gtrsim 2$ mJy), the peak of the differential counts is made mainly by $0.5 \lesssim z \lesssim 1.5$ sources, although at $S_{24\,\mu m} \lesssim 0.16$ mJy (corresponding roughly to the limit of the deepest, nonlensed, ISOCAM survey: $S_{15\,\mu m} = 0.12$ mJy; see Fig. 5) the higher z

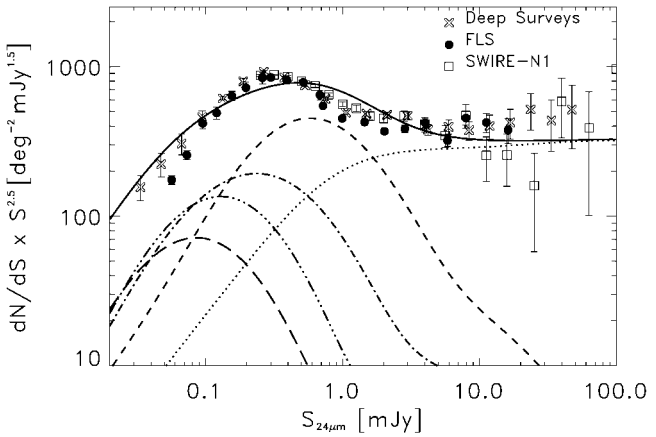

FIG. 5.—Differential redshift contribution to the normalized differential source counts at 24 μm. The dotted, dashed, dot-dashed, triple-dot–dashed, and long-dashed lines correspond to the 0.0–0.5, 0.5–1.0, 1.0–1.5, 1.5–2.0, and 2.0–2.5 redshift intervals, respectively.

population contributes for a conspicuous fraction (~46%). By extrapolating the source counts model down to the faintest fluxes, we obtain an estimate of the total 24 μm background: $\nu I_\nu(24\ \mu\mathrm{m}) \sim 2.4$ nW m^{-2} sr^{-1}. According to our model, the amount produced by sources at $z \lesssim 1.5$ is ~1.6 nW m^{-2} sr^{-1}; therefore, ~66% of the 24 μm background originates at relatively low redshift. From the comparison between the total background predicted by our model and the value derived from the observed 24 μm source counts (1.9 ± 0.6 nW m^{-2} sr^{-1}; Papovich et al. 2004), we find that the *Spitzer* deep surveys already resolve ~78% of the total 24 μm background.

3.2. *Observed ISOCAM Counts Transformed to* 24 μm

To compare observed data counts at 15 μm with those at 24 μm, we have converted the 15 μm source counts obtained from different ISOCAM surveys (from the ultradeep lensed of Metcalfe et al. 2003, to the shallower ELAIS survey of Gruppioni et al. 2002) to 24 μm, as described in the following text. We have convolved the observed 15 μm differential counts ($dN/dS_{15\,\mu\mathrm{m}}$) with the distribution of the ratios $S_{24\,\mu\mathrm{m}}/S_{15\,\mu\mathrm{m}}$ obtained from our model, given a 15 μm source selection ($f[(S_{24\,\mu\mathrm{m}}/S_{15\,\mu\mathrm{m}}), S_{15\,\mu\mathrm{m}}]$):

$$dN(S_{24\,\mu\mathrm{m}}) = \int f\left(\frac{S_{24\,\mu\mathrm{m}}}{S_{15\,\mu\mathrm{m}}}, S_{15\,\mu\mathrm{m}}\right) \frac{dN}{dS_{15\,\mu\mathrm{m}}}(S_{15\,\mu\mathrm{m}}) dS_{15\,\mu\mathrm{m}}. \quad (2)$$

Data at 15 μm from different samples have been combined by weighting each point by its formal error (inverse of the squared error). In Figure 3, the counts derived from the 15 μm observed data (*shaded area*) are overplotted to the 24 μm data and model. The two different source counts are consistent and, in first approximation, seem to agree well. In particular, at high flux densities we do not observe the discrepancy as reported by Marleau et al. (2004), thanks to a more accurate flux density ratio applied. On the other hand, the discrepancy observed at 24 μm fluxes lower than ~0.05 mJy is only apparent, since fluxes fainter than this are not sampled by the 15 μm data. Some level of inconsistency between the two source counts are visible around ~1 mJy, where the 15 μm counts (and the model) are higher than the observed 24 μm source counts. A decrease of the $S_{24\,\mu\mathrm{m}}/S_{15\,\mu\mathrm{m}}$ ratio around 1 mJy could be obtained by slightly modifying the starburst template in the MIR range (i.e., increasing the PAH features with respect to the continuum, since at the typical redshift of sources with these flux densities, $z \approx 1$, the PAH features enter the 15 μm band). A similar change was made by Lagache et al. (2004), who show how a minor change in the starburst template spectra between 12 and 30 μm (together with a slight modification of the luminosity density) was a sufficient a posteriori modification to enable a model not fitting the observed 24 μm source counts (Lagache et al. 2003) to reproduce the observations.

We are actually working at improving the model-data agreement by including also the recently published 24 μm source counts (and all the MIR-FIR counts and redshift distributions available in literature) as an observational constraint to the maximum likelihood analysis of our 15 μm–based model. Moreover, we are considering the use of an SED library, with different SEDs associated not only to different populations but also to different luminosity classes (i.e., Chary & Elbaz 2001). The model improvements will be described in a future paper (F. Pozzi et al. 2005, in preparation), since they are beyond the scope of the present Letter, whose intent is just to show, through a simple 15 μm–based model, what the 24 μm/15 μm comparison can tell us in terms of galaxy evolutionary properties.

4. CONCLUSIONS

We have discussed the importance of a comparison between the extragalactic source counts in two different MIR bands for the study of the evolutionary properties of galaxies. We have shown what we expect in terms of variations of the $S_{24\,\mu\mathrm{m}}/S_{15\,\mu\mathrm{m}}$ flux density ratio with redshift and 24 μm flux, considering typical SEDs for the different populations contributing to the source counts. Then, to compare the observed *Spitzer* 24 μm source counts with the ISOCAM 15 μm ones, we have presented the prediction in the 24 μm *Spitzer* band from a phenomenological evolution model based on the ISOCAM 15 μm LF of galaxies and AGNs. Actually, this model is the only one available in literature that is able to reproduce the observed 24 μm source counts without the need, at least in first approximation, of any a posteriori updates. We have also shown that the observed ISOCAM data points transformed from 15 to 24 μm seem to agree well with the recently published *Spitzer* source counts. Our model suggests the appearance of a new population of high-redshift ($z > 1.5$) galaxies at 24 μm, not detected in the previous ISOCAM surveys but probably the high-z likes of the 15 μm sources.

We thank the anonymous referee for valuable comments that improved the quality of this Letter and D. L. Shupe and I. Matute for kindly providing SWIRE data counts and AGN models before publication.

REFERENCES

Chary, R., & Elbaz, D. 2001, ApJ, 556, 562
Chary, R., et al. 2004, ApJS, 154, 80
Elbaz, D., Cesarsky, C. J., Chanial, P., Aussel, H., Franceschini, A. Fadda, D., & Chary, R. 2002, A&A, 384, 848
Elbaz, D., et al. 1999, A&A, 351, L37
Elvis, M., et al. 1994, ApJS, 95, 1
Förster Schreiber, N. M., Sauvage, M., Charmandaris, V., Laurent, O., Gallais, P., Mirabel, I. F., & Vigroux, L. 2003, A&A, 399, 833
Franceschini, A., Aussel, H., Cesarsky, C. J., Elbaz, D., & Fadda, D. 2001, A&A, 378, 1
Gruppioni, C., Lari, C., Pozzi, F., Zamorani, G., Franceschini, A., Oliver, S., Rowan-Robinson, M., & Serjeant, S. 2002, MNRAS, 335, 831
Hauser, M. G., & Dwek, E. 2001, ARA&A, 39, 249
La Franca, F., et al. 2004, AJ, 127, 3075
Lagache, G., Dole, H., & Puget, J.-L. 2003, MNRAS, 338, 555
Lagache, G., et al. 2004, ApJS, 154, 112
Lari, C., et al. 2001, MNRAS, 325, 1173
Marshall, H. L., et al. 1983, ApJ, 269, 35
Marleau, F., et al. 2004, ApJS, 154, 66
Metcalfe, L., et al. 2003, A&A, 407, 791
Papovich, C., et al. 2004, ApJS, 154, 70
Puget, J.-L., & Leger, A. 1989, ARA&A, 27, 161
Pozzi, F., et al. 2004, ApJ, 609, 122
Rodighiero, G., et al. 2004, A&A, 427, 773
Roussel, H., et al. 2001, A&A, 369, 473
Rowan-Robinson, M., et al. 2004, MNRAS, 351, 1290
Rush, B., Malkan, M. A., & Spinoglio, L. 1993, ApJS, 89, 1
Silva, L., et al. 1998, ApJ, 509, 103
Sturm, E., Lutz, D., Tran, D., Feuchtgruber, H., Genzel, R., Kunze, D., Moorwood, A. F. M., & Thornley, M. D. 2000, A&A, 358, 481